

Analytic theory of stochastic oscillations in single-cell gene expression

Chen Jia^{1,*}, Hong Qian², Michael Q. Zhang³

¹ Applied and Computational Mathematics Division, Beijing Computational Science Research Center, Beijing 100193, China.

³ Department of Applied Mathematics, University of Washington, Seattle, WA 98195, U.S.A.

² Department of Biological Sciences, University of Texas at Dallas, Richardson, TX 75080, U.S.A.

* Correspondence: chenjia@csrc.ac.cn

Abstract

Noise-induced oscillations in individual cells are usually characterized by a non-monotonic power spectrum with an oscillatory autocorrelation function. Here we develop an analytical approach of stochastic oscillations in a minimal stochastic gene expression model including promoter state switching, protein synthesis and degradation, as well as a genetic feedback loop. The autocorrelated function, power spectrum, and probability distribution of protein concentration fluctuations are computed in closed form. Using the solvable model, we illustrate oscillations as a stochastic circulation along a hysteresis loop. A triphasic stochastic bifurcation upon the increasing strength of negative feedback is observed, which reveals how stochastic bursts evolve into stochastic oscillations. Translational bursting is found to enhance the robustness and broaden the region of stochastic oscillations in our model. These results provide deeper insights into R. Thomas' two conjectures for single-cell stochastic gene expression kinetics.

1 Introduction

The engineering concept of feedback loops has been extremely useful in understanding non-linear biological dynamics [1] and cellular regulations [2] in terms of biochemical kinetics [3]. In connection to gene regulatory networks, René Thomas proposed two conjectures in 1981 [4]: (i) The presence of a positive feedback loop is a necessary condition for multiple stable states; (ii) The presence of a negative feedback loop is a necessary condition for sustained oscillations. Many efforts since then have been devoted to the investigation and proof of these two conjectures. However, the majority of previous studies are based on deterministic models of continuous and discrete dynamical systems, such as ordinary differential equations (ODEs) and Boolean networks. In the context of continuous dynamical systems, both the first and second conjectures have been extensively studied based on the concept of local or global interaction graph [5–10].

Over the past two decades, large amounts of single-cell experiments, some with single-molecule sensitivity, have revealed a large cell-to-cell variation in the numbers of mRNA and protein molecules in isogenic populations due to stochasticity in gene expression and the low copy numbers of many components, including DNA and important regulatory molecules [11–15]. To explain noisy experimental data, notable breakthroughs have been made in the kinetic theory of single-cell stochastic gene expression [16, 17]. The stochastic properties of gene regulation have been explored mostly by stochastic simulations and to a lesser extent by analytical solutions of various discrete, continuous, and hybrid gene expression models. Discrete models are those in which the numbers of genes, mRNAs, and proteins change by discrete integer amounts when reactions occur [18]. In continuous models, fluctuations correspond to hops on the real axis rather than on the integer axis [19–23]. In hybrid models, the fluctuations of genes are modeled discretely, while the fluctuations of mRNAs and proteins are modeled in a continuous sense [24–32]. Here we focus on the hybrid model since (i) it serves as an accurate approximation of

the discrete model when molecule numbers are relatively large [31, 32], and (ii) the protein abundance is usually modelled as a continuous variable in previous studies on oscillations.

Sustained oscillations are common in nature. Most previous studies about biological oscillations are based on deterministic modelling and analysis [33–35]. Some of the best-understood biological oscillators include p53 responses [36–38], NF- κ B responses [39–41], cell cycle [42, 43], circadian rhythm [44, 45], calcium spikes [46, 47], and various synthetic oscillators [48–50]. However, there are growing observations that gene expression in single cells can display stochastic oscillations, and noise can play a vital role in enhancing or weakening the robustness of these oscillations [51, 52]. Statistically, noise-induced oscillations are usually quantified by a non-monotonic power spectrum [53, 54] with an oscillatory autocorrelation function [55–57]. In recent years, significant progress has been made in the analytical theory of stochastic oscillations in single-cell gene expression, where the autocorrelation function and power spectrum of protein concentration fluctuations are computed and analyzed [58–64]. However, these studies are often based on various simplifying assumptions and hence are not exact. For example, both quantities have been approximately obtained in a negative feedback loop with delayed protein synthesis under the assumption that the time delay is large compared to other characteristic times of the system [58]. Thus far, there is still a lack of an exact theory of stochastic oscillations at the single-cell level; also, there is a lack of an in-depth understanding of Thomas’ conjectures in the context of stochastic gene expression with feedback controls.

In this paper, we develop an analytical approach and present a comprehensive analysis for stochastic oscillations in a minimal stochastic gene expression model with promoter state switching, protein synthesis and degradation, as well as a genetic feedback loop. The structure of the present paper is as follows. In Sec. 2, we describe our hybrid ODE model in detail, and also derive the dynamic equations of low order moments. In Sec. 3, we derive the analytical expressions of the autocorrelation function and power spectrum of protein concentration fluctuations, and also compute the dominant frequency and oscillatory efficiency when oscillations are present. Moreover, we reveal the emergence of a triphasic stochastic bifurcation as the negative feedback strength increases. In Sec. 4, we compute the probability distribution of protein concentrations, and also provide an intuitive and mechanistic picture of Thomas’ two conjectures for single-cell stochastic gene expression. With this picture, sustained oscillations are shown to be as a stochastic circulation along a hysteresis loop. In Sec. 5, we compute the autocorrelation function and power spectrum exactly in a more complex hybrid model, which takes protein bursting into account. We investigate the influence of burstiness on our model in detail and find that protein bursting enhances the robustness and broaden the region of stochastic oscillations. We conclude in Sec. 6.

2 Model

Gene regulatory networks can be tremendously complex, involving numerous signaling steps and genetic feedback loops. However, the situation becomes much simpler if we focus on a particular gene and the feedback loop regulating it [65]. In general, there are three types of gross feedback topologies for the gene of interest: no feedback, positive feedback, and negative feedback (Fig. 1(a)). Here we consider a minimal stochastic gene expression model that can produce sustained oscillations. The model includes synthesis and degradation of the protein, as well as switching of the gene between an active and an inactive state (Fig. 1(b)). The evolution of the protein concentration x is usually modeled as a hybrid ODE [24–30], also called a piecewise deterministic Markov process:

$$\begin{aligned} \dot{x} &= \rho - dx && \text{(active state),} \\ a(x) &\Downarrow b(x) \\ \dot{x} &= -dx && \text{(inactive state),} \end{aligned}$$

where ρ is the synthesis rate of the protein when the gene is in the active state, and d is the degradation rate of the protein. There is no protein synthesis when the gene is in the inactive state. Due to feedback regulation, the protein concentration x will directly or indirectly affect the switching rates $a(x)$ and $b(x)$ of the gene between the two

states. There are two reasons why we use a hybrid ODE to model oscillations in gene expression. First, the hybrid model has been shown to be an accurate approximation of the discrete chemical master equation (CME) model when the protein number is relatively large [31, 32], which is a result of the system size expansion. Second, the protein abundance is usually modelled as a continuous variable in previous studies on oscillations, and hence we use the hybrid model instead of the CME model where the protein abundance is modelled discretely.

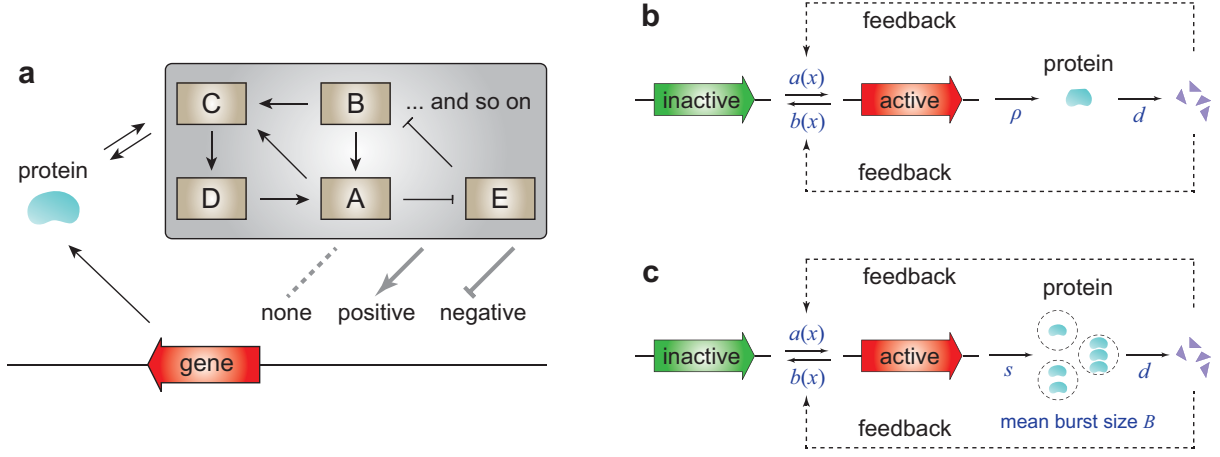


Figure 1: **Schematics of stochastic gene expression in living cells.** (a) Three types of gross feedback topologies. Gene regulatory networks in a living cell can be extremely complex, involving numerous feedback loops and signaling steps (grey box). If we focus on a particular gene of interest (red), then there are three types of fundamental regulatory relations: no feedback (none), positive feedback, and negative feedback. The dotted line represents that there is no link between adjacent nodes. (b) Two-state model of gene expression involving gene state switching, protein synthesis, and protein degradation. Due to feedback regulation, the switching rates between the active and inactive gene states, $a(x)$ and $b(x)$, depend on the protein concentration x . Here protein synthesis occurs in a non-bursty manner. (c) Two-state model of gene expression involving gene state switching, protein synthesis, and protein degradation. Here protein synthesis occurs in a bursty manner.

Clearly, if the gene is unregulated, then the gene switching rates $a(x) = a$ and $b(x) = b$ are constants independent of the protein concentration x . In a positive (negative) feedback network, the gene activation rate $a(x)$ is an increasing (decreasing) function of x due to epigenetic controls such as association (dissociation) of activators, while the gene inactivation rate $b(x)$ is an decreasing (increasing) function of x due to epigenetic controls such as dissociation (association) of repressors. To establish an analytic theory of stochastic oscillations in single cells, we assume that $a(x)$ and $b(x)$ are linear with respect to x :

$$a(x) = a - ux, \quad b(x) = b + ux, \quad (1)$$

where $|u|$ characterizes the strength of feedback regulation with $u = 0$ corresponding to unregulated genes, $u > 0$ corresponding to negatively regulated genes, and $u < 0$ corresponding to positively regulated genes. The functional forms of $a(x)$ and $b(x)$ introduced above are essentially consistent with a popular model for NF- κ B nuclear translocation, a most well-understood biological oscillator [66]. Such linear dependence of $a(x)$ and $b(x)$ on x has been widely used in the study of autoregulatory gene circuits [67–71]. However, most previous studies allow only one of $a(x)$ and $b(x)$ to be dependent on x , while the other is a constant. Here we require both $a(x)$ and $b(x)$ to be dependent on x .

The microstate of the gene can be represented by an ordered pair (i, x) , where i is the gene state with $i = 0, 1$ corresponding to the inactive and active states, respectively. Let $p_i(x, t)$ denote the probability density of the protein concentration at time t when the gene is in state i . Then the evolution of the hybrid ODE model is governed by the Kolmogorov forward equation

$$\begin{cases} \partial_t p_0 = d\partial_x(xp_0) + b(x)p_1 - a(x)p_0, \\ \partial_t p_1 = d\partial_x(xp_1) - \rho\partial_x p_1 + a(x)p_0 - b(x)p_1. \end{cases} \quad (2)$$

To proceed, let $p_{\text{on}}(t) = \int_0^\infty p_1(x, t) dx$ denote the probability of the gene being in the active state at time t and let $m(t) = \langle x(t) \rangle$ denote the mean protein concentration, where $x(t)$ is the protein concentration in a single cell at time t . Using Eq. (2), the active probability $p_{\text{on}}(t)$ and mean protein concentration $m(t)$ satisfy the following system of ODEs (see Appendix A for the proof):

$$\frac{d}{dt} \begin{pmatrix} p_{\text{on}}(t) \\ m(t) \end{pmatrix} = -T \begin{pmatrix} p_{\text{on}}(t) \\ m(t) \end{pmatrix} + \begin{pmatrix} a \\ 0 \end{pmatrix}, \quad (3)$$

where T is a matrix defined by

$$T = \begin{pmatrix} a + b & u \\ -\rho & d \end{pmatrix}.$$

The two eigenvalues λ_1 and λ_2 of the matrix T are the solutions to the quadratic equation

$$\lambda^2 - (d + a + b)\lambda + d(a + b) + \rho u = 0,$$

which has a discriminant $\Delta = (d - a - b)^2 - 4\rho u$. We assume that the gene network can reach a steady state, which implies that both λ_1 and λ_2 have positive real parts. Clearly, if the gene is unregulated or positively regulated, then $u \leq 0$ and thus $\Delta > 0$, which shows that the two eigenvalues are both positive real numbers.

3 Analytical autocorrelation function and power spectrum

The oscillations in a stochastic system are usually characterized by the autocorrelation function and power spectrum. The former $C(t) = \text{Cov}_{ss}(x(0), x(t))$ is defined as the steady-state covariance of $x(0)$ and $x(t)$, and the latter $G(\omega) = \int_{-\infty}^{\infty} C(|t|) e^{-2\pi i \omega t} dt$ is defined as the Fourier transform of $C(|t|)$. In general, sustained oscillations cannot be observed if $G(\omega)$ is monotonically decreasing over $[0, \infty)$, while a non-monotonic $G(\omega)$ over $[0, \infty)$ serves as a characteristic signal of robust stochastic oscillations with the maximum point being the dominant frequency. It is easy to check that the autocorrelation function can be represented as

$$C(t) = \sum_{i=0}^1 \int_0^\infty x p_i(x, \infty) [m_i(x, t) - m_i(x, \infty)] dx,$$

where $m_i(x, t)$ is the conditional mean of protein concentration at time t given that the initial gene state is i and the initial protein concentration is x . Solving Eq. (3) with appropriate initial conditions, we can obtain exact formulas of $m_0(x, t)$ and $m_1(x, t)$. In this way, the autocorrelation function $C(t)$ can also be calculated analytically. Taking the Fourier transform of $C(|t|)$ gives the analytic expression of the power spectrum $G(\omega)$.

If the gene is unregulated, then the two eigenvalues of the matrix T are given by $\lambda_1 = a + b$ and $\lambda_2 = d$. In this case, both $C(t)$ and $G(\omega)$ can be calculated explicitly as (see Appendix B for the proof)

$$C(t) = \frac{\rho^2 ab}{d(a+b)^2(d+a+b)} \left[\frac{de^{-(a+b)t} - (a+b)e^{-dt}}{d-a-b} \right], \quad (4)$$

$$G(\omega) = \frac{2\rho^2 ab}{(a+b)(4\pi^2\omega^2 + d^2)[4\pi^2\omega^2 + (a+b)^2]},$$

where $C(t)$ is a linear combination of two exponential functions. This result is in full agreement with a recent single-cell experiment on nuclear localization of Crz1 protein in response to extracellular calcium, where the authors found that at calcium concentrations greater than 100 mM, the autocorrelation function of localization trajectories is better fit by a sum of two exponentials [73]. In addition, our result also shows that the weights of the two exponential functions have opposite signs, which suggests that the gene network is in a nonequilibrium steady state. This is because if a Markovian system is in equilibrium, then the autocorrelation function must be a linear combination of exponential functions with nonpositive coefficients [74]. From Eq. (4), it is easy to check that $C(t)$ and $G(\omega)$ are both monotonically decreasing.

In a positive feedback network, similar computations show that (see Appendix B for the proof)

$$\begin{aligned} C(t) &= K \left[\frac{\lambda_1 e^{-\lambda_2 t} - \lambda_2 e^{-\lambda_1 t}}{\lambda_1 - \lambda_2} \right], \\ G(\omega) &= \frac{2K \lambda_1 \lambda_2 (\lambda_1 + \lambda_2)}{(4\pi^2 \omega^2 + \lambda_1^2)(4\pi^2 \omega^2 + \lambda_2^2)}, \end{aligned} \quad (5)$$

where

$$K = \frac{\rho^2 da(db + \rho u)}{[d(a + b) + \rho u]^2 [d(d + a + b) + \rho u]} \quad (6)$$

is a constant. Recall that λ_1 and λ_2 are positive real numbers in the presence of a positive feedback loop. This shows that both $C(t)$ and $G(\omega)$ are still monotonically decreasing. Hence robust oscillations fail to be observed if the gene is unregulated or positively regulated.

More interesting is the situation of negative feedback networks. In the presence of a negative feedback loop, the discriminant $\Delta = (d - a - b)^2 - 4\rho u$ may become negative. In particular, the negative feedback strength u has a critical value

$$u_s = \frac{(d - a - b)^2}{4\rho}.$$

If $u \leq u_s$, then $\Delta \geq 0$ and thus λ_1 and λ_2 are positive real numbers. In this case, both $C(t)$ and $G(\omega)$ have the form of Eq. (5) and are monotonically decreasing. If $u > u_s$, then $\Delta < 0$ and λ_1 and λ_2 become conjugated complex numbers. For convenience, we represent them as $\lambda_1 = \alpha - \beta i$ and $\lambda_2 = \alpha + \beta i$, where $\alpha, \beta > 0$. In this case, the autocorrelation function exhibits a damped oscillation and thus must be non-monotonic:

$$C(t) = K e^{-\alpha t} \cos(\beta t - \phi),$$

where $K > 0$ is the constant given in Eq. (6) and the phase ϕ satisfies $\tan \phi = \alpha/\beta$. Moreover, the power spectrum is given by

$$G(\omega) = \frac{2K(\alpha \cos \phi + \beta \sin \phi)(\alpha^2 + \beta^2)}{[\alpha^2 + (2\pi\omega - \beta)^2][\alpha^2 + (2\pi\omega + \beta)^2]}. \quad (7)$$

It is easy to show that $G(\omega)$ is non-monotonic if and only if (the absolute value of) the imaginary part of λ_1 and λ_2 exceeds the real part, i.e. $\beta > \alpha$. Straightforward computations show that

$$\beta^2 - \alpha^2 = \frac{1}{2}[2\rho u - (a + b)^2 - d^2].$$

Therefore, there is another critical value

$$u_c = \frac{(a + b)^2 + d^2}{2\rho} > u_s = \frac{(d - a - b)^2}{4\rho}$$

for the negative feedback strength u . If $u_s < u \leq u_c$, then $\beta \leq \alpha$ and $G(\omega)$ must be monotonically decreasing. In this case, although the autocorrelation displays a damped oscillation, the power spectrum is still monotonic and thus oscillations cannot be observed. If $u > u_c$, then $\beta > \alpha$ and thus $G(\omega)$ becomes non-monotonic. In particular, a negative feedback network with inversely correlated gene switching rates can exhibit robust oscillations when the feedback strength is sufficiently large. In this case, $G(\omega)$ attains its maximum at

$$\omega = \frac{\sqrt{\beta^2 - \alpha^2}}{2\pi} = \frac{\sqrt{\rho(u - u_c)}}{2\pi},$$

which can be understood as the intrinsic frequency of sustained oscillations. It is clear that both a large degradation rate d or a large total gene switching rate $a + b$ will result in a large critical value u_c for the feedback strength.

We have now provided a complete characterization of the oscillatory behavior of stochastic gene expression in three types of gene networks. If the gene is unregulated or positively regulated, both $C(t)$ and $G(\omega)$ are monotonic, and thus no oscillations could be observed. However, a stochastic bifurcation will occur if the gene is negatively

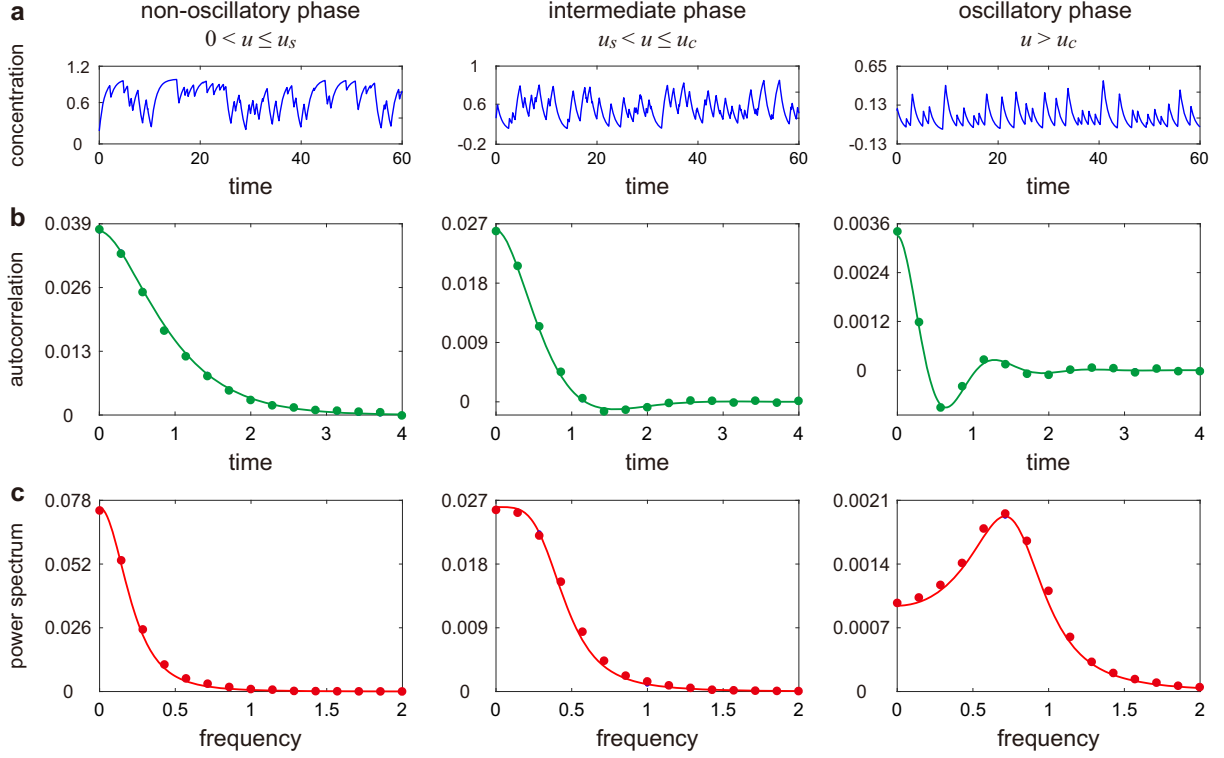


Figure 2: **Stochastic bifurcations of oscillations in negative feedback networks.** The negative feedback strength u has two critical values u_s and u_c , which separate the parameter region into three phases: the non-oscillatory phase of $0 < u \leq u_s$, the transitional phase of $u_s < u \leq u_c$, and the oscillatory phase of $u > u_c$. **(a)** Typical trajectory of the protein concentration in the three phases. **(b)** Autocorrelation functions of the protein concentration in the three phases. **(c)** Power spectra of the protein concentration in the three phases. In (b),(c), the curve shows the analytical solution given in Eq. (5), and the dots show the simulated results. The model parameters in (a)-(c) are chosen as $a = 3, b = 0, \rho = d = 1$. The negative feedback strength is chosen to be $u = u_s$ in the non-oscillatory phase, $u = u_c$ in the transitional phase, and $u = 5u_c$ in the oscillatory phase.

regulated. To gain an intuitive picture of this, we simulate the trajectories of the hybrid model under three sets of biologically relevant parameters and then use them to compute $C(t)$ and $G(\omega)$ (Fig. 2(a)-(c)). The numerical power spectrum is computed by means of the Wiener-Khinchin theorem, which states that $G(\omega) = \lim_{T \rightarrow \infty} \langle |\hat{n}_T(\omega)|^2 \rangle / T$, where $\hat{n}_T(\omega) = \int_0^T n(t) e^{-2\pi i \omega t} dt$ is the truncated Fourier transform of a single stochastic trajectory over the interval $[0, T]$ and the angled brackets denote the ensemble average over trajectories. In fact, the two critical values of the negative feedback strength, u_s and u_c , separate the parameter region into three phases. In the non-oscillatory phase of $u \leq u_s$, both $C(t)$ and $G(\omega)$ are monotonic. In the transitional phase of $u_s < u \leq u_c$, the former becomes non-monotonic while the latter is still monotonic. In the oscillatory phase of $u > u_c$, both quantities become non-monotonic. Note that when the protein is very stable ($d \approx 0$), the critical value $u_c = (a + b)^2 / 2\rho$ separating the transitional and oscillatory phases is twice the critical value $u_s = (a + b)^2 / 4\rho$ separating the transitional and non-oscillatory phases.

Let G_{peak} denote the peak value of the power spectrum. To evaluate the performance of stochastic oscillations, we define a quantity called *oscillatory efficiency*:

$$\eta = \frac{G_{\text{peak}} - G(0)}{G_{\text{peak}}} = 1 - \frac{G(0)}{G_{\text{peak}}},$$

which is a number between 0 and 1. Clearly, a large value of η implies that the spectrum at the dominant frequency is much larger than the spectrum at zero frequency, which means that oscillations are strong. If $G(\omega)$ is monotonically decreasing, then $G_{\text{peak}} = G(0)$ and thus η vanishes. Hence the efficiency η serves as an effective indicator that describes the robustness of oscillations. When $u > u_c$, the efficiency can be computed explicitly as

$$\eta = 1 - \left[\frac{2\alpha\beta}{\alpha^2 + \beta^2} \right]^2 = \left[\frac{2\rho(u - u_c)}{(d + a + b)^2 + 2\rho(u - u_c)} \right]^2.$$

As the negative feedback strength u increases, the efficiency η becomes larger and thus oscillations become more apparent (Fig. 2(a)).

Experimentally, the single-cell tracks of gene expression always fluctuate stochastically around the mean. For such time-lapse data, it is sometimes difficult to distinguish whether the underlying dynamics belongs to stochastic bursts [75] or stochastic oscillations. This issue has been pointed out in a recent single-cell experiment on nuclear localization of Crz1 protein [73], where the authors found that at very high calcium levels, the stochastic bursts of Crz1 nuclear localization trajectories look similar to sustained oscillations. In fact, our theory leads to a clear distinction between stochastic bursts ($u \leq u_c$) and stochastic oscillations ($u > u_c$). Typically, stochastic bursts do not have an intrinsic frequency and thus give rise to a monotonic power spectrum, whereas stochastic oscillations have an intrinsic period and are featured by a non-monotonic power spectrum. Thus for time-lapse gene expression data, a simple way of determining the underlying dynamics is to estimate the power spectrum and identify its monotonicity.

Thus far, our analytic theory is developed under the assumption that both the gene switching rates linearly depend on the protein concentration and are inversely correlated (Eq. (1)). However, our main results are actually insensitive to the specific functional forms of $a(x)$ and $b(x)$ except their monotonicity. More generally, we may assume that $a(x) = a - vx$ and $b(x) = b + ux$, where u and v are two constants jointly characterizing the feedback strength. In this case, it is almost impossible to obtain the analytic solutions of $C(t)$ and $G(\omega)$. However, according to our simulations, a negative feedback network also undergoes a stochastic bifurcation as u and v increases while keeping u/v as a constant. Furthermore, robust oscillations can also be observed when $a(x)$ and $b(x)$ are chosen to be non-linear Michaelis-Menten or Hill functions with opposite monotonicity, and oscillations become stronger as the cooperativity in the Hill function increases (Fig. 3). Unfortunately, we find that no sustained oscillations could be observed if $a(x) = a$ is a constant and $b(x) = b + ux$, an assumption imposed on many models of autorepressive genes [69]. This indicates that an oversimple regulation mechanism may not be sufficient to yield robust oscillations.

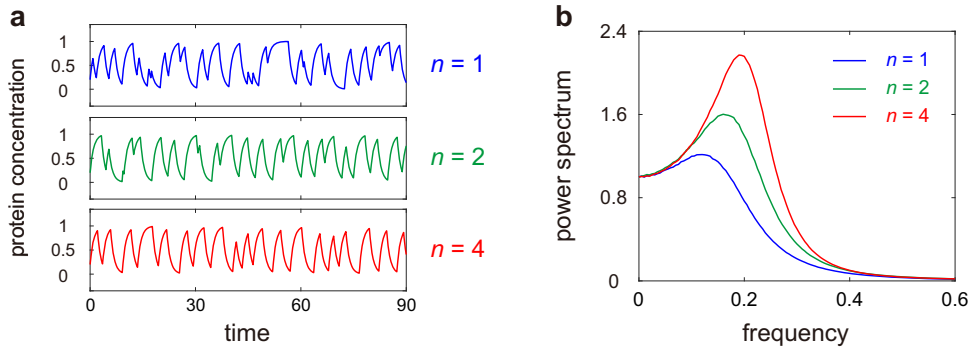


Figure 3: **Oscillations when gene switching rates depend non-linearly on the protein concentration.** Here the gene switching rates are chosen as Hill functions $a(x) = a/[1 + (ux)^n]$ and $b(x) = a/[1 + (u(w-x))^n]$, where $w = \rho/d$ is the maximum protein concentration and u is the strength of negative feedback. Note that when the cooperativity n is large, $a(x)$ transitions sharply from a to 0 around $x = 1/u$, while $b(x)$ transitions sharply from 0 to a around $x = w - 1/u$ (see Fig. 4(b) for an illustration). (a) Typical trajectories of the protein concentration when $n = 1, 2, 4$. (b) Simulated power spectra of the protein concentration when $n = 1, 2, 4$. Here the spectra are normalized so that $G(0) = 1$. The model parameters in (a),(b) are chosen as $a = \rho = d = 1, u = 5$.

4 Deeper understanding of Thomas' conjectures

Our stochastic model can also be applied to gain a deeper understanding of Thomas' first conjecture. By solving Eq. (2), we can obtain the steady-state probability density of the protein concentration, which turns out to

be a beta distribution (see Appendix C for the proof):

$$p_{ss}(x) = \frac{\Gamma(\beta)w^{1-\beta}}{\Gamma(\alpha)\Gamma(\beta-\alpha)}x^{\alpha-1}(w-x)^{\beta-\alpha-1}, \quad x < w, \quad (8)$$

where $w = \rho/d$ is the maximum protein concentration, and α and β are two constants given by

$$\alpha = \frac{a}{d}, \quad \beta = \frac{a+b}{d} + \frac{\rho u}{d^2}.$$

Note that when $u = 0$, our model reduces to the hybrid ODE model of gene expression for unregulated genes and it has long been proved that the protein concentration has a beta distribution in this special case [24–26]. Our results generalize this result to regulated genes ($u \neq 0$).

In fact, the steady-state protein distribution can be either unimodal or bimodal. From (8), bimodality occurs if and only if $a < d$ and

$$u < \frac{d(d-b)}{\rho}. \quad (9)$$

In particular, for unregulated genes, we have $u = 0$ and thus gene expression displays bimodality if and only if both gene switching rates are slower than the degradation rate, i.e. $a < d$ and $b < d$. In fact, a similar result has been proved for the discrete CME model of gene expression [76]. This suggests that Thomas’ first conjecture is not always true in living organisms: bimodality can occur in unregulated or even negatively regulated networks when the gene switches slowly between the active and inactive states [18]. Furthermore, when the gene inactivation rate is greater than or equal to the degradation rate, i.e. $b \geq d$, the right side of Eq. (9) is nonpositive and thus bimodality can only take place in positive feedback networks, which reinforces Thomas’ first conjecture.

Thomas’ two conjectures can be understood intuitively using the schematic diagrams depicted in Fig. 4. Since the gene switching rates $a(x)$ and $b(x)$ have opposite monotonicity in positive and negative feedback networks, the stable and unstable regions for the active and inactive states are also different in the two types of networks, each forming a hysteresis loop. Here stable and unstable regions are defined as regions with slow and fast gene switching rates, respectively. In the presence of positive feedback, the stable attractors of the two gene states lie in the stable regions, forming bimodality (Fig. 4(a)). In the presence of negative feedback, however, the stable attractors lie in the unstable regions. Before the protein level could approach a stable attractor, it has already entered the unstable region and thus will switch to the other gene state. With time, the protein level will fluctuate around the hysteresis loop, forming sustained oscillations (Fig. 4(b)). This understanding not only provides a theoretical complement to previous computational studies on relaxation oscillators, where similar hysteretic switch was found [34], but also is supported by previous experimental studies, which showed that the response of many cell cycle regulatory elements in *Xenopus* are hysteretic [77].

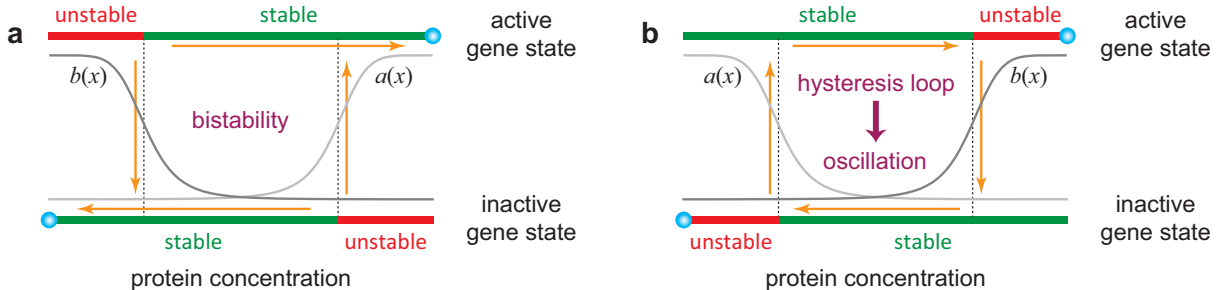


Figure 4: **Schematics of the Markovian dynamics in positive and negative feedback networks.** (a) Positive feedback networks. (b) Negative feedback networks. The upper and lower layers represent the active and inactive states of the gene. The light and dark grey curves illustrate the graphs of the gene switching rates $a(x)$ and $b(x)$, respectively. The blue balls show the locations of the stable attractors for the two gene states. The stable and unstable regions for the two gene states are depicted as green and red bars, respectively. The yellow arrows indicate the evolution direction of the Markovian dynamics.

5 Generalization to systems with bursty protein synthesis

Interestingly, our main results are also robust with respect to the specific gene expression model used. In some previous studies [31, 32], the evolution of the protein concentration x is modeled as a hybrid stochastic differential equation (SDE):

$$\begin{aligned} \dot{x} &= \dot{\xi}_t - dx && \text{(active state),} \\ a(x) \uparrow \Big| \Big| b(x) \\ \dot{x} &= -dx && \text{(inactive state).} \end{aligned}$$

where ξ_t is a compound Poisson process capturing the bursty production of protein (Fig. 1(c)). The jump rate of ξ_t corresponds to the burst frequency and the jump distribution of ξ_t corresponds to the burst size distribution. Note that when the gene is always active and the burst size has an exponential distribution, this model reduces to the classical bursty model of gene expression proposed in [19] (also see [20–23]). Recently, it has been shown [31, 32] that the hybrid ODE and SDE models can be viewed as different macroscopic limits of the discrete CME model of stochastic gene expression as the size of the system tends to infinity. The former performs better in the regime of large burst frequencies, while the latter performs better in the regime of large burst sizes.

The evolution of the hybrid SDE model is governed by the Kolmogorov forward equation

$$\begin{cases} \partial_t p_0 = d\partial_x(xp_0) + b(x)p_1 - a(x)p_0, \\ \partial_t p_1 = d\partial_x(xp_1) + s\mu * p_1 + a(x)p_0 - [b(x) + s]p_1, \end{cases} \quad (10)$$

where s is the burst frequency, $\mu(dx)$ is the burst size distribution, and $\mu * p_1(x) = \int_0^x p_1(x-y)\mu(dy)$ denotes the convolution of μ and p_1 . In previous studies [19], the burst size distribution is often chosen to be the exponential distribution $\mu(dx) = \lambda e^{-\lambda x} dx$, which is supported by single-molecule experiments [13]. If the gene is unregulated, both the autocorrelation function $C(t)$ and power spectrum $G(\omega)$ can be calculated explicitly as (see Appendix D for the proof)

$$C(t) = \widehat{C}(t) + \widetilde{C}(t), \quad G(\omega) = \widehat{G}(\omega) + \widetilde{G}(\omega), \quad (11)$$

where $\widehat{C}(t)$ and $\widehat{G}(\omega)$ are defined as in Eq. (4) with $\rho = sB$, and

$$\widetilde{C}(t) = \frac{as\sigma}{2d(a+b)} e^{-dt}, \quad \widetilde{G}(\omega) = \frac{as\sigma}{(a+b)(4\pi^2\omega^2 + d^2)}$$

with $\sigma = \int_0^\infty x^2 \mu(dx)$ being the second moment of the burst size distribution. In this case, both $C(t)$ and $G(\omega)$ are the sums of two monotonically decreasing functions. This leads to the same conclusion that oscillations cannot be observed if the gene is unregulated, even if protein bursting is taken into account.

In the presence of feedback loops, $C(t)$ and $G(\omega)$ can also be calculated analytically as

$$C(t) = c_1 e^{-\lambda_1 t} + c_2 e^{-\lambda_2 t}, \quad G(\omega) = \frac{2c_1 \lambda_1}{4\pi^2 \omega^2 + \lambda_1^2} + \frac{2c_2 \lambda_2}{4\pi^2 \omega^2 + \lambda_2^2}, \quad (12)$$

where c_1 and c_2 can be determined by solving the following two equations

$$\begin{aligned} c_1 + c_2 &= \frac{2\rho^2 da(db + \rho u) + das\sigma(d + a + b)[d(a + b) + \rho u]}{2[d(a + b) + \rho u]^2 [d(d + a + b) + \rho u]}, \\ \lambda_1 c_1 + \lambda_2 c_2 &= \frac{das\sigma}{2[d(a + b) + \rho u]}, \end{aligned} \quad (13)$$

with $\rho = sB$ being the effective synthesis rate of the protein. In this case, the correlation function (power spectrum) is still the weighted sum of two exponential (Lorentzian) functions, but the weights are much more complicated than those in the hybrid ODE model. Straightforward computations show that the expressions of $C(t)$ and $G(\omega)$ in the bursty case (Eq. (12)) reduce to those in the non-bursty case (Eq. (5)) when the second moment of the burst size distribution vanishes, i.e. $\sigma = 0$.

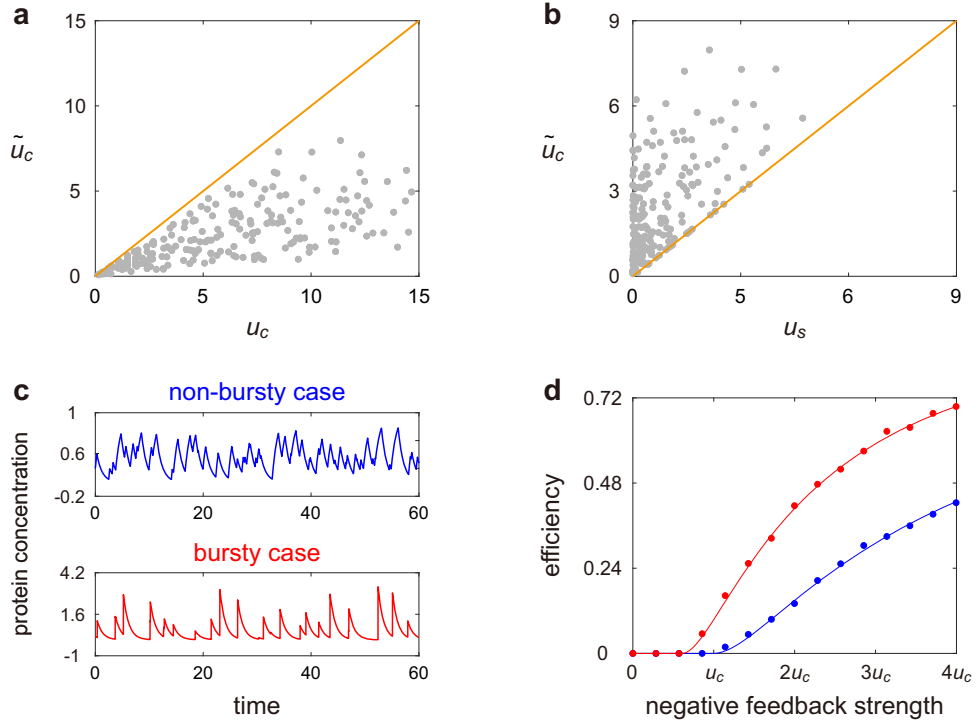


Figure 5: **Comparison of stochastic oscillations in the non-bursty and bursty cases.** Stochastic bifurcations of oscillations can be observed in both the non-bursty and bursty models. In the bursty case, the burst size is chosen to be exponentially distributed. **(a)** Scatter plot of \tilde{u}_c versus u_c , where \tilde{u}_c is critical value of oscillations in the bursty model. **(b)** Scatter plot of \tilde{u}_c versus u_s . In (a),(b), we randomly sample 200 sets of model parameters. Specifically, the model parameters are randomly chosen as $a \sim U[0, 10]$, $b \sim U[0, 1]$, $s \sim U[0, 10]$, $sB \sim U[1, 10]$, $d \sim U[0, 10]$, where $U[x, y]$ denotes the uniform distribution over the interval $[x, y]$. **(c)** Typical trajectories for the non-bursty and bursty models when $u = u_c$. **(d)** Oscillatory efficiencies for the non-bursty (blue) and bursty (red) models as a function of the negative feedback strength u . In (c),(d), the curves show theoretical results and the dots show simulated ones. The model parameters are chosen as $a = 3, b = 0, d = 1$ in both the non-bursty and bursty cases, $\rho = 1$ in the non-bursty case, and $s = B = 1$ in the bursty case.

To compare the oscillatory behaviors of the hybrid ODE and SDE models, we choose model parameters so they share the same mean field dynamics. Based on our simulations, we find that stochastic bifurcations take place in both models. However, for the hybrid SDE model, it is almost impossible to compute the explicit expression of the critical value. Interestingly, we find that the critical value of oscillations \tilde{u}_c (the critical value separating monotonic and non-monotonic power spectra) in the bursty case is always smaller than its counterpart u_c in the non-bursty case, suggesting that the hybrid SDE model requires a smaller negative feedback strength u to generate robust oscillations than the hybrid ODE model. To see this, we randomly select 200 sets of model parameters and compute the values of u_s , u_c and \tilde{u}_c under each set of parameters (the explicit expression of power spectrum given in Eq. (12) allows us to compute the value of \tilde{u}_c without simulating the trajectories). Fig. 5(a),(b) illustrate the scatter plots of \tilde{u}_c versus u_c and u_s . It is clear that for all sets of parameters, \tilde{u}_c is always smaller than u_c and is always larger than u_s .

Fig. 5(c) illustrates the typical trajectories of the two models when $u = u_c$. It is clear that oscillations fail to be observed at the critical value u_c for the hybrid ODE model, while the hybrid SDE model displays much more apparent oscillations. To reinforce this result, we depict the oscillatory efficiencies of the two models in Fig. 5(d) as a function of the negative feedback strength u . Under the model parameters chosen, the critical value in the bursty case is only $0.6u_c$, and for a fixed feedback strength u , the hybrid SDE model possesses a much higher efficiency. All these results reveal that burstiness in protein production is expected to boost the occurrence and broaden the region of stochastic oscillations, while it gives rise to larger gene expression noise [16]. A reasonable explanation for this counterintuitive result is that a single burst will drive the protein abundance to jump from a low to a much higher value. This helps the system cross the boundary more easily from the stable region for the active

gene state to the unstable region, as illustrated in Fig. 4(b). Once the burst occurs, the gene will switch rapidly from the active to the inactive state and then the protein abundance will decay to a lower value again to finish a cycle. Hence protein bursting plays an important role in prolonging the cycle times and enhancing the robustness of oscillations (Fig. 5(c)). We emphasize that while protein bursting promotes oscillations in our model, it may destroy oscillations in other systems — it has been shown that burstiness may either promote or destroy oscillations in more complex networks involving autocatalysis, trimerization, and feedback loops [52]. Stochasticity increasing the robustness of oscillations has been discussed earlier in [51].

6 Conclusions and discussion

In this paper, we provide an analytical approach of stochastic oscillations in a minimal model of single-cell stochastic gene expression which includes promoter state switching, protein synthesis and degradation, as well as a genetic feedback loop. The positive or negative feedback is modelled as linear dependence of the gene activation and inactivation rates on the protein concentration with opposite monotonicity. The evolution of the protein concentration is modelled as a piecewise-deterministic Markov process. Within this framework, we computed the autocorrelation function, power spectrum, and probability distribution of concentration fluctuations in closed form in the presence of feedback regulation. The autocorrelation function (power spectrum) turns out to be the weighted sum of two exponential (Lorentzian) functions with the weights having opposite signs. The protein concentration has a beta distribution in steady state.

Using the analytical results, we reinforced previous results that robust oscillations fail to be observed when the gene is unregulated or positively regulated since the two exponential components do not have an imaginary part. More interestingly, we found that a negative feedback network undergoes a triphasic stochastic bifurcation with the increase of the feedback strength: the autocorrelation function first changes from a monotonic to a non-monotonic curve at a small critical value due to the emergence of imaginary parts of the two exponential components, and then the power spectrum changes from a monotonic to a non-monotonic curve at a larger critical value due to the competition of the real and imaginary parts of the two exponential components. The two critical values separate the parameter region into an non-oscillatory phase with monotonic autocorrelation and spectrum, a transitional phase with non-monotonic autocorrelation and monotonic spectrum, and an oscillatory phase with non-monotonic autocorrelation and spectrum. In the oscillatory phase, we also calculated the analytical expressions of the dominating frequency and oscillatory efficiency. Based on simulations, we further showed that similar stochastic bifurcations can also be observed when the gene switching rates depend non-linearly on the protein concentration, and oscillations become stronger as the cooperativity in the Hill function increases.

Our model and analytical results allow us to gain deeper insights into Thomas' two conjectures. We showed that Thomas' first conjecture is not always true in living organisms: bimodality can occur in unregulated or even negatively regulated networks when promoter state switching is taken into account. However, when the gene inactivation rate is greater than or equal to the protein degradation rate, we showed that bimodality can only take place in positive feedback networks, which reinforces Thomas' first conjecture in this special case. In addition, our model also provides an intuitive understanding of Thomas' two conjectures. Since the gene switching rates have opposite dependence on the protein concentration in positive and negative feedback networks, the two gene states also have different stable and unstable regions in the two types of networks, each forming a hysteresis loop. In the presence of positive feedback, the attractors for the two gene states lie in the stable regions, forming bimodality. In the presence of negative feedback, the attractors for the two gene states lie in the unstable regions; in this case, the protein level will fluctuate around the hysteresis loop, forming sustained oscillations.

Finally, we investigated the influence of protein bursting on stochastic oscillations by modelling protein synthesis as a compound Poisson process with the jump rate corresponding to the burst frequency and with the jump distribution corresponding to the burst size distribution. This yields a hybrid stochastic differential equation model of concentration fluctuations. Similarly to the non-bursty case, we computed the analytical expressions of

the autocorrelation function and power spectrum when protein bursting is taken into account. Based on theory and simulations, we showed that the critical value of oscillations in the bursty case is always lower than its counterpart in the non-bursty case. Moreover, when the feedback strength is fixed, the bursty model always produces a higher oscillatory efficiency than the non-bursty model. These results reveal that burstiness in protein production will broaden the region and enhance the robustness of stochastic oscillations in our model.

In summary, there are growing observations showing that gene expression in single cells can display stochastic oscillations [36–41, 48], which are distinct from random fluctuations and should be quantified by a non-monotonic power spectrum [53, 54] with an oscillatory autocorrelation function [55–57], or be understood as a circular random walk or stochastic flow [51, 78]. Although negative feedback is widely suspected to be necessary based on deterministic dynamics [4], more mechanistic nature of this phenomenon is still largely unknown. Our analytic theory shows that a negative feedback loop with inversely correlated gene switching rates can result in a stochastic bifurcation evolving from stochastic bursts to stochastic oscillations for single-cell gene expression. In the oscillatory regime, the essence of stochastic oscillations is revealed to be a circular motion along a stochastic hysteresis loop. Even though translational bursts yield large gene expression noise, it can enhance the robustness of stochastic oscillations. Further elucidations of the biochemical steps for negative feedback loops in specific cells are expected. We also anticipate that the analytical method developed in this paper can be generalized to more complex gene regulatory networks [61, 64].

Appendices

A. Derivation of the moment equations

Note that the active probability $p_{\text{on}}(t)$ and mean protein concentration $m(t)$ can be represented as

$$p_{\text{on}}(t) = \int_0^\infty p_1(x, t) dx, \quad m(t) = \int_0^\infty xp(x, t) dx$$

where $p(x, t) = p_0(x, t) + p_1(x, t)$ is the probability density of the protein concentration at time t . Integrating the second equation of Eq. (2), we obtain

$$\begin{aligned} \frac{d}{dt} p_{\text{on}}(t) &= \int_0^\infty \partial_t p_1 dx = \int_0^\infty [(a - ux)p_0 - (b + ux)p_1] dx \\ &= \int_0^\infty (ap_0 - bp_1 - uxp) dx \\ &= a[1 - p_{\text{on}}(t)] - bp_{\text{on}}(t) - um(t) \\ &= a - (a + b)p_{\text{on}}(t) - um(t). \end{aligned}$$

Similarly, using Eq. (2) and integration by parts, we obtain

$$\begin{aligned} \frac{d}{dt} m(t) &= \int_0^\infty x \partial_t p dx = \int_0^\infty x [d\partial_x(xp) - \rho\partial_x p_1] dx \\ &= \int_0^\infty (\rho p_1 - dxp) dx \\ &= \rho p_{\text{on}}(t) - dm(t). \end{aligned}$$

Hence $p_{\text{on}}(t)$ and $m(t)$ satisfy the system of ODEs given in Eq. (3). This system of ODEs holds generally for any initial distribution of the Markovian model. The time-dependent solution of this system of ODEs is given by

$$\begin{pmatrix} p_{\text{on}}(t) \\ m(t) \end{pmatrix} = e^{-Tt} \begin{pmatrix} p_{\text{on}}(0) \\ m(0) \end{pmatrix} + (I - e^{-Tt})T^{-1} \begin{pmatrix} a \\ 0 \end{pmatrix}.$$

Let $m_i(x, t)$ denote the conditional mean of the protein concentration at time t given that the initial gene state is i and the initial protein concentration is x . Then we have

$$\begin{pmatrix} p_{\text{on}}(t) \\ m_i(x, t) \end{pmatrix} = e^{-Tt} \begin{pmatrix} i \\ x \end{pmatrix} + (I - e^{-Tt})T^{-1} \begin{pmatrix} a \\ 0 \end{pmatrix}.$$

Hence $m_i(x, t)$ can be computed explicitly as

$$m_i(x, t) = (0, 1)e^{-Tt} \begin{pmatrix} i \\ x \end{pmatrix} + (0, 1)(I - e^{-Tt})T^{-1} \begin{pmatrix} a \\ 0 \end{pmatrix}. \quad (14)$$

B. Derivation of the correlation function and power spectrum

We next compute the analytical expressions of the correlation function and power spectrum. To this end, let

$$r(t) = \int_0^\infty xp_1(x, t)dx$$

denote the unnormalized mean of the protein concentration at time t when the gene is active and let

$$s(t) = \int_0^\infty x^2p(x, t)dx$$

denote the second moment of the protein concentration at time t . Then we have

$$\begin{aligned} \frac{d}{dt}r(t) &= \int_0^\infty x\partial_t p_1 dx = \int_0^\infty x[d\partial_x(xp_1) - \rho\partial_x p_1 + (a - ux)p_0 - (b + ux)p_1]dx \\ &= \int_0^\infty (\rho p_1 - dxp_1 + axp_0 - bxp_1 - ux^2p)dx \\ &= \rho p_{\text{on}}(t) + am(t) - (d + a + b)r(t) - us(t). \end{aligned}$$

Similarly, we have

$$\begin{aligned} \frac{d}{dt}s(t) &= \int_0^\infty x^2\partial_t p dx = \int_0^\infty x^2[d\partial_x(xp) - \rho\partial_x p_1]dx \\ &= 2 \int_0^\infty (\rho xp_1 - dx^2p)dx \\ &= 2\rho r_1(t) - 2ds(t). \end{aligned}$$

This shows that

$$\frac{d}{dt} \begin{pmatrix} r(t) \\ s(t) \end{pmatrix} = -R \begin{pmatrix} r(t) \\ s(t) \end{pmatrix} + \begin{pmatrix} \rho p_{\text{on}}(t) + am(t) \\ 0 \end{pmatrix}, \quad (15)$$

where R is a matrix defined by

$$R = \begin{pmatrix} d + a + b & u \\ -2\rho & 2d \end{pmatrix}. \quad (16)$$

In steady state, it follows from Eq. (3) that

$$\begin{pmatrix} p_{\text{on}}(\infty) \\ m(\infty) \end{pmatrix} = T^{-1} \begin{pmatrix} a \\ 0 \end{pmatrix} = \frac{a}{d(a+b) + \rho u} \begin{pmatrix} d \\ \rho \end{pmatrix}. \quad (17)$$

This shows that

$$\rho p_{\text{on}}(\infty) + am(\infty) = \frac{\rho a(a+d)}{d(a+b) + \rho u}.$$

Moreover, using Eq. (3) again shows that

$$\begin{aligned} \begin{pmatrix} r(\infty) \\ s(\infty) \end{pmatrix} &= R^{-1} \begin{pmatrix} \rho p_{\text{on}}(\infty) + am(\infty) \\ 0 \end{pmatrix} \\ &= \frac{\rho a(a+d)}{[d(a+b) + \rho u][d(d+a+b) + \rho u]} \begin{pmatrix} d \\ \rho \end{pmatrix}. \end{aligned} \quad (18)$$

To proceed, let $\alpha(t)$ denote the gene state and let $x(t)$ denote the protein concentration in an individual cell at time t , respectively. Note that $\alpha(t)$ and $x(t)$ are stochastic processes. Given the initial state $\alpha(0) = i$ and initial protein concentration $x(0) = x$, it follows from Eq. (14) that

$$\mathbb{E}x(t) = (0, 1)e^{-Tt} \begin{pmatrix} i \\ x \end{pmatrix} + (0, 1)(I - e^{-Tt})T^{-1} \begin{pmatrix} a \\ 0 \end{pmatrix}.$$

This clearly shows that

$$\mathbb{E}[x(t)|\alpha(0), x(0)] = (0, 1)e^{-Tt} \begin{pmatrix} \alpha(0) \\ x(0) \end{pmatrix} + (0, 1)(I - e^{-Tt})T^{-1} \begin{pmatrix} a \\ 0 \end{pmatrix}.$$

Hence, in steady state, we have

$$\begin{aligned} \mathbb{E}x(0)x(t) &= \sum_{i=0}^1 \mathbb{E}x(0)I_{\{\alpha(0)=i\}}\mathbb{E}[x(t)|\alpha(0), x(0)] \\ &= \sum_{i=0}^1 \mathbb{E}x(0)I_{\{\alpha(0)=i\}} \left[(0, 1)e^{-Tt} \begin{pmatrix} \alpha(0) \\ x(0) \end{pmatrix} + (0, 1)(I - e^{-Tt})T^{-1} \begin{pmatrix} a \\ 0 \end{pmatrix} \right] \\ &= (0, 1)e^{-Tt} \begin{pmatrix} r(\infty) \\ s(\infty) \end{pmatrix} + m(\infty)(0, 1)(I - e^{-Tt})T^{-1} \begin{pmatrix} a \\ 0 \end{pmatrix}. \end{aligned}$$

Note that the correlation function is given by $C(t) = \mathbb{E}x(0)x(t) - \mathbb{E}x(0)\mathbb{E}x(t)$. Then we finally obtain the explicit expression of the correlation function, which is given by

$$C(t) = (0, 1)e^{-Tt} \begin{pmatrix} r(\infty) \\ s(\infty) \end{pmatrix} + m(\infty)(0, 1)(I - e^{-Tt})T^{-1} \begin{pmatrix} a \\ 0 \end{pmatrix} - m(\infty)^2. \quad (19)$$

Taking $t = 0$ in the above equation and applying Eqs. (17) and (18) yield

$$C(0) = s(\infty) - m(\infty)^2 = \frac{\rho^2 da(db + \rho u)}{[d(a+b) + \rho u]^2[d(d+a+b) + \rho u]}.$$

Moreover, taking the derivative on both sides of Eq. (19) shows that

$$C'(t) = -(0, 1)e^{-Tt}T \begin{pmatrix} r(\infty) \\ s(\infty) \end{pmatrix} + m(\infty)(0, 1)e^{-Tt} \begin{pmatrix} a \\ 0 \end{pmatrix}.$$

Taking $t = 0$ in the above equation yields

$$C'(0) = -(0, 1)T \begin{pmatrix} r(\infty) \\ s(\infty) \end{pmatrix} = 0,$$

where we have used the fact that

$$T \begin{pmatrix} r(\infty) \\ s(\infty) \end{pmatrix} = 0,$$

which follows easily from Eq. (18). This shows that the correlation function for the hybrid ODE model must have zero derivative at $t = 0$. Without loss of generality, we assume that the eigenvalues of the matrix T are distinct. In fact, any matrix can be approximated by such matrices to any degree of accuracy. It then follows from Eq. (19) that

$$C(t) = c_1 e^{-\lambda_1 t} + c_2 e^{-\lambda_2 t},$$

where λ_1 and λ_2 are the two eigenvalues of the matrix T . Since $C'(0) = 0$, we obtain

$$\lambda_1 c_1 + \lambda_2 c_2 = 0.$$

Thus the correlation function has the following analytical expression:

$$C(t) = K \left[\frac{\lambda_1 e^{-\lambda_2 t} - \lambda_2 e^{-\lambda_1 t}}{\lambda_1 - \lambda_2} \right],$$

where

$$K = C(0) = \frac{\rho^2 da(db + \rho u)}{[d(a + b) + \rho u]^2 [d(d + a + b) + \rho u]}$$

is a constant. Taking the Fourier transform gives the following analytical expression of the power spectrum:

$$G(\omega) = \frac{2K \lambda_1 \lambda_2 (\lambda_1 + \lambda_2)}{(4\pi^2 \omega^2 + \lambda_1^2)(4\pi^2 \omega^2 + \lambda_2^2)}.$$

This is exactly Eq. (5) in the main text.

If the gene is unregulated, then we have $u = 0$ and the two eigenvalues of the matrix T are given by $\lambda_1 = a + b$ and $\lambda_2 = d$. This gives Eq. (4) in the main text.

C. Derivation of the steady-state protein distribution

Let $p_i^{ss}(x)$ denote the steady-state probability density of the protein concentration when the gene is in state i , and let $p^{ss}(x) = p_0^{ss}(x) + p_1^{ss}(x)$. In steady state, adding the two equations in Eq. (2) yields

$$\frac{d}{dx} [dx p_0^{ss} - (\rho - dx) p_1^{ss}] = 0.$$

This shows that

$$dx p_0^{ss} - (\rho - dx) p_1^{ss} = K,$$

where K is a constant. Note that p_0^{ss} and p_1^{ss} must decay exponentially as $x \rightarrow \infty$. Taking $x \rightarrow \infty$ in the above equation shows that $K = 0$. Hence we have $(\rho - dx) p_1^{ss}(x) = dx p_0^{ss}(x)$. For convenience, we set

$$\psi(x) = (\rho - dx) p_1^{ss}(x) = dx p_0^{ss}(x).$$

Moreover, it follows from Eq. (2) that

$$\psi'(x) = a(x) p_0^{ss}(x) - b(x) p_1^{ss}(x) = \left[\frac{a(x)}{dx} - \frac{b(x)}{\rho - dx} \right] \psi(x).$$

Integrating the above equation gives

$$\psi(x) = C \exp \left\{ \int_1^x \left[\frac{a(y)}{dy} - \frac{b(y)}{\rho - dy} \right] dy \right\}, \quad (20)$$

where C is a normalization constant. Finally, the steady-state probability density of the protein concentration is given by

$$p^{ss}(x) = p_0^{ss}(x) + p_1^{ss}(x) = \left[\frac{1}{dx} + \frac{1}{\rho - dx} \right] \psi(x). \quad (21)$$

Computing the integral in Eq. (20) explicitly and inserting the resulting $\psi(x)$ into Eq. (21) gives Eq. (8) in the main text.

D. Derivation of the autocorrelation function and power spectra in the bursty case

The computation of the autocorrelation function and power spectra for the hybrid SDE model follows the same line as that for the hybrid ODE model. Integrating the second equation of Eq. (10), we obtain

$$\begin{aligned}
\frac{d}{dt}p_{\text{on}}(t) &= \int_0^\infty \partial_t p_1 dx = s \int_0^\infty \mu * p_1 dx + \int_0^\infty [(a - ux)p_0 - (b + s + ux)p_1] dx \\
&= s \int_0^\infty \mu(dy) \int_y^\infty p_1(x - y, t) dx + \int_0^\infty [ap_0 - (b + s)p_1 - uxp] dx \\
&= sp_{\text{on}}(t) + a[1 - p_{\text{on}}(t)] - (b + s)p_{\text{on}}(t) - um(t) \\
&= a - (a + b)p_{\text{on}}(t) - um(t).
\end{aligned}$$

Similarly, using Eq. (10) and integration by parts, we obtain

$$\begin{aligned}
\frac{d}{dt}m(t) &= \int_0^\infty x \partial_t p dx = \int_0^\infty x [d \partial_x (xp) + s\mu * p_1 - sp_1] dx \\
&= s \int_0^\infty \mu(dy) \int_y^\infty xp_1(x - y, t) dx - s \int_0^\infty p_1 dx - d \int_0^\infty xp dx \\
&= s \int_0^\infty \mu(dy) \int_0^\infty (x + y)p_1(x, t) dx - s \int_0^\infty p_1 dx - d \int_0^\infty xp dx \\
&= \rho p_{\text{on}}(t) - dm(t),
\end{aligned}$$

where $\rho = s \int_0^\infty y\mu(dy)$ is the product of the burst frequency and mean burst size. In this case, $p_{\text{on}}(t)$ and $m(t)$ also satisfy the system of ODEs given in Eq. (3). Let $m_i(x, t)$ denote the conditional mean of the protein concentration at time t given that the initial gene state is i and the initial protein concentration is x . Then $m_i(x, t)$ can be computed explicitly as in Eq. (14).

To proceed, let

$$r(t) = \int_0^\infty xp_1(x, t) dx, \quad s(t) = \int_0^\infty x^2 p(x, t) dx.$$

Then we have

$$\begin{aligned}
\frac{d}{dt}r(t) &= \int_0^\infty x \partial_t p_1 dx = \int_0^\infty x [d \partial_x (xp_1) + s\mu * p_1 + (a - ux)p_0 - (b + s + ux)p_1] dx \\
&= \int_0^\infty [sx\mu * p_1 - dxp_1 + axp_0 - (b + s)xp_1 - ux^2p] dx \\
&= \rho p_{\text{on}}(t) + am(t) - (d + a + b)r(t) - us(t).
\end{aligned}$$

Similarly, we have

$$\begin{aligned}
\frac{d}{dt}s(t) &= \int_0^\infty x^2 \partial_t p dx = \int_0^\infty x^2 [d \partial_x (xp) + s\mu * p_1 - sp_1] dx \\
&= s \int_0^\infty \mu(dy) \int_y^\infty x^2 p_1(x - y, t) dx - s \int_0^\infty x^2 p_1 dx - 2d \int_0^\infty x^2 p dx \\
&= s \int_0^\infty \mu(dy) \int_0^\infty (x + y)^2 p_1(x, t) dx - s \int_0^\infty x^2 p_1 dx - 2d \int_0^\infty x^2 p dx \\
&= 2\rho \int_0^\infty xp_1(x, t) dx + s \int_0^\infty y^2 \mu(dy) \int_0^\infty p_1(x, t) dx - 2d \int_0^\infty x^2 p dx \\
&= 2\rho r(t) + \gamma p_{\text{on}}(t) - 2ds(t),
\end{aligned}$$

where $\gamma = s \int_0^\infty y^2 \mu(dy)$ is the product of the burst frequency and the second moment of the burst size. This shows that

$$\frac{d}{dt} \begin{pmatrix} r(t) \\ s(t) \end{pmatrix} = -R \begin{pmatrix} r(t) \\ s(t) \end{pmatrix} + \begin{pmatrix} \rho p_{\text{on}}(t) + am(t) \\ \gamma p_{\text{on}}(t) \end{pmatrix}, \quad (22)$$

where R is the matrix given in Eq. (16). Note that in the bursty case, the above equation is different from Eq. (15) in the non-bursty case. In steady state, it follows from Eq. (3) that

$$\begin{aligned} \begin{pmatrix} r(\infty) \\ s(\infty) \end{pmatrix} &= R^{-1} \begin{pmatrix} \rho p_{\text{on}}(\infty) + am(\infty) \\ \gamma p_{\text{on}}(\infty) \end{pmatrix} = R^{-1} \begin{pmatrix} \rho & a \\ \gamma & 0 \end{pmatrix} T^{-1} \begin{pmatrix} a \\ 0 \end{pmatrix} \\ &= \frac{1}{2[d(a+b) + \rho u][d(d+a+b) + \rho u]} \begin{pmatrix} 2\rho da(d+a) - dau\gamma \\ 2\rho^2 a(d+a) + da\gamma(d+a+b) \end{pmatrix}. \end{aligned} \quad (23)$$

Similarly to the proof in the non-bursty case, the autocorrelation function $C(t)$ has the form of

$$C(t) = (0, 1)e^{-Tt} \begin{pmatrix} r(\infty) \\ s(\infty) \end{pmatrix} + m(\infty)(0, 1)(I - e^{-Tt})T^{-1} \begin{pmatrix} a \\ 0 \end{pmatrix} - m(\infty)^2. \quad (24)$$

Taking $t = 0$ in the above equation and applying Eqs. (17) and (23) yield

$$C(0) = s(\infty) - m(\infty)^2 = \frac{2\rho^2 da(db + \rho u) + da\gamma(d+a+b)[d(a+b) + \rho u]}{2[d(a+b) + \rho u]^2[d(d+a+b) + \rho u]}.$$

Moreover, taking the derivative on both sides of Eq. (24) shows that

$$C'(t) = -(0, 1)e^{-Tt}T \begin{pmatrix} r(\infty) \\ s(\infty) \end{pmatrix} + m(\infty)(0, 1)e^{-Tt} \begin{pmatrix} a \\ 0 \end{pmatrix}.$$

Taking $t = 0$ in the above equation yields

$$C'(0) = -(0, 1)T \begin{pmatrix} r(\infty) \\ s(\infty) \end{pmatrix} = -\frac{da\gamma}{2[d(a+b) + \rho u]}.$$

This shows that the correlation function for the hybrid SDE model may have negative derivative at $t = 0$. Without loss of generality, we assume that the eigenvalues of the matrix T are distinct. In fact, any matrix can be approximated by such matrices to any degree of accuracy. It then follows from Eq. (24) that

$$C(t) = c_1 e^{-\lambda_1 t} + c_2 e^{-\lambda_2 t},$$

where λ_1 and λ_2 are the two eigenvalues of the matrix T . Note that

$$c_1 + c_2 = C(0) = \frac{2\rho^2 da(db + \rho u) + da\gamma(d+a+b)[d(a+b) + \rho u]}{2[d(a+b) + \rho u]^2[d(d+a+b) + \rho u]}, \quad (25)$$

and we also have

$$\lambda_1 c_1 + \lambda_2 c_2 = -C'(0) = \frac{da\gamma}{2[d(a+b) + \rho u]}. \quad (26)$$

Then c_1 and c_2 can be calculated by solving the above two equations. This gives the closed-form expression of the autocorrelation function. Taking the Fourier transform gives the following analytical expression of the power spectrum:

$$G(\omega) = \frac{2c_1 \lambda_1}{4\pi^2 \omega^2 + \lambda_1^2} + \frac{2c_2 \lambda_2}{4\pi^2 \omega^2 + \lambda_2^2}.$$

This gives Eq. (12) in the main text.

If the gene is unregulated, then we have $u = 0$ and the two eigenvalues of the matrix T are given by $\lambda_1 = a + b$ and $\lambda_2 = d$. In this case, solving Eqs. (25) and (26) shows that

$$\begin{aligned} c_1 &= \frac{\rho^2 ab}{(a+b)^2(d+a+b)(d-a-b)}, \\ c_2 &= -\frac{\rho^2 ab}{d(a+b)(d+a+b)(d-a-b)} + \frac{a\gamma}{2d(a+b)}. \end{aligned}$$

This gives Eq. (11) in the main text.

Acknowledgements

We thank Ramon Grima, X. Sunney Xie, and Xuejuan Zhang for stimulating discussions and for sharing unpublished results. C. J. acknowledges support from National Natural Science Foundation of China (NSFC) with NSAF grant No. U2230402, grant No. 12131005, and grant No. 12271020. H. Q. thanks partial support from the Olga Jung Wan Endowed Professorship. M. Q. Z. acknowledges support from NIH with grant No. MH102616 and grant No. MH109665, and also by NSFC with grant No. 31671384 and grant No. 91329000.

References

- [1] Murray, J. D. *Mathematical Biology: I. An Introduction* (Springer, New York, 2007), 3rd edn.
- [2] Alon, U. *An Introduction to Systems Biology: Design Principles of Biological Circuits* (Chapman and Hall, New York, 2006).
- [3] Qian, H. Cooperativity in cellular biochemical processes: Noise-enhanced sensitivity, fluctuating enzyme, bistability with nonlinear feedback, and other mechanisms for sigmoidal responses. *Annu. Rev. Biophys.* **41**, 179–204 (2012).
- [4] Thomas, R. On the relation between the logical structure of systems and their ability to generate multiple steady states or sustained oscillations. In *Numerical Methods in the Study of Critical Phenomena*, 180–193 (Springer, 1981).
- [5] Plahte, E., Mestl, T. & Omholt, S. W. Feedback loops, stability and multistationarity in dynamical systems. *J. Biol. Syst.* **3**, 409–413 (1995).
- [6] Gouzé, J.-L. Positive and negative circuits in dynamical systems. *J. Biol. Syst.* **6**, 11–15 (1998).
- [7] Snoussi, E. H. Necessary conditions for multistationarity and stable periodicity. *J. Biol. Syst.* **6**, 3–9 (1998).
- [8] Cinquin, O. & Demongeot, J. Positive and negative feedback: striking a balance between necessary antagonists. *J. Theor. Biol.* **216**, 229–242 (2002).
- [9] Soulé, C. Graphic requirements for multistationarity. *ComplexUs* **1**, 123–133 (2003).
- [10] Richard, A. & Comet, J.-P. Stable periodicity and negative circuits in differential systems. *J. Math. Biol.* **63**, 593–600 (2011).
- [11] Elowitz, M. B., Levine, A. J., Siggia, E. D. & Swain, P. S. Stochastic gene expression in a single cell. *Science* **297**, 1183–1186 (2002).
- [12] Golding, I., Paulsson, J., Zawilski, S. M. & Cox, E. C. Real-time kinetics of gene activity in individual bacteria. *Cell* **123**, 1025–1036 (2005).
- [13] Cai, L., Friedman, N. & Xie, X. S. Stochastic protein expression in individual cells at the single molecule level. *Nature* **440**, 358–362 (2006).
- [14] Raj, A. & van Oudenaarden, A. Nature, nurture, or chance: stochastic gene expression and its consequences. *Cell* **135**, 216–226 (2008).
- [15] Taniguchi, Y. *et al.* Quantifying E. coli proteome and transcriptome with single-molecule sensitivity in single cells. *Science* **329**, 533–538 (2010).
- [16] Paulsson, J. Models of stochastic gene expression. *Phys. Life Rev.* **2**, 157–175 (2005).
- [17] Schnoerr, D., Sanguinetti, G. & Grima, R. Approximation and inference methods for stochastic biochemical kinetics — a tutorial review. *J. Phys. A: Math. Theor.* **50**, 093001 (2017).
- [18] Shahrezaei, V. & Swain, P. S. Analytical distributions for stochastic gene expression. *Proc. Natl. Acad. Sci. USA* **105**, 17256–17261 (2008).
- [19] Friedman, N., Cai, L. & Xie, X. S. Linking stochastic dynamics to population distribution: an analytical framework of gene expression. *Phys. Rev. Lett.* **97**, 168302 (2006).
- [20] Mackey, M. C., Tyran-Kaminska, M. & Yvinec, R. Dynamic behavior of stochastic gene expression models in the presence of bursting. *SIAM J. Appl. Math.* **73**, 1830–1852 (2013).
- [21] Bokes, P. & Singh, A. Protein copy number distributions for a self-regulating gene in the presence of decoy binding sites. *PLoS one* **10**, e0120555 (2015).
- [22] Jedrak, J. & Ochab-Marcinek, A. Time-dependent solutions for a stochastic model of gene expression with molecule production in the form of a compound Poisson process. *Phys. Rev. E* **94**, 032401 (2016).
- [23] Chen, X. & Jia, C. Limit theorems for generalized density-dependent Markov chains and bursty stochastic gene regulatory networks. *J. Math. Biol.* **80**, 959–994 (2020).

- [24] Karmakar, R. & Bose, I. Graded and binary responses in stochastic gene expression. *Phys. Biol.* **1**, 197 (2004).
- [25] Raj, A., Peskin, C. S., Tranchina, D., Vargas, D. Y. & Tyagi, S. Stochastic mRNA synthesis in mammalian cells. *PLoS Biol.* **4**, e309 (2006).
- [26] Dattani, J. & Barahona, M. Stochastic models of gene transcription with upstream drives: exact solution and sample path characterization. *J. R. Soc. Interface* **14**, 20160833 (2017).
- [27] Ge, H., Qian, H. & Xie, X. S. Stochastic phenotype transition of a single cell in an intermediate region of gene state switching. *Phys. Rev. Lett.* **114**, 078101 (2015).
- [28] Newby, J. Bistable switching asymptotics for the self-regulating gene. *J. Phys. A: Math. Theor.* **48**, 185001 (2015).
- [29] Lin, Y. T. & Doering, C. R. Gene expression dynamics with stochastic bursts: Construction and exact results for a coarse-grained model. *Phys. Rev. E* **93**, 022409 (2016).
- [30] Bressloff, P. C. Stochastic switching in biology: from genotype to phenotype. *J. Phys. A: Math. Theor.* **50**, 133001 (2017).
- [31] Jia, C., Zhang, M. Q. & Qian, H. Emergent Levy behavior in single-cell stochastic gene expression. *Phys. Rev. E* **96**, 040402(R) (2017).
- [32] Jia, C., Yin, G. G., Zhang, M. Q. *et al.* Single-cell stochastic gene expression kinetics with coupled positive-plus-negative feedback. *Phys. Rev. E* **100**, 052406 (2019).
- [33] Novák, B. & Tyson, J. J. Design principles of biochemical oscillators. *Nat. Rev. Mol. Cell Biol.* **9**, 981–991 (2008).
- [34] Tsai, T. Y.-C. *et al.* Robust, tunable biological oscillations from interlinked positive and negative feedback loops. *Science* **321**, 126–129 (2008).
- [35] Li, Z., Liu, S. & Yang, Q. Incoherent inputs enhance the robustness of biological oscillators. *Cell Syst.* **5**, 72–81 (2017).
- [36] Lev Bar-Or, R. *et al.* Generation of oscillations by the p53-Mdm2 feedback loop: a theoretical and experimental study. *Proc. Natl. Acad. Sci. USA* **97**, 11250–11255 (2000).
- [37] Lahav, G. *et al.* Dynamics of the p53-Mdm2 feedback loop in individual cells. *Nat. Genet.* **36**, 147 (2004).
- [38] Geva-Zatorsky, N. *et al.* Oscillations and variability in the p53 system. *Mol. Syst. Biol.* **2** (2006).
- [39] Hoffmann, A., Levchenko, A., Scott, M. L. & Baltimore, D. The I κ B-NF- κ B signaling module: temporal control and selective gene activation. *Science* **298**, 1241–1245 (2002).
- [40] Nelson, D. *et al.* Oscillations in NF- κ B signaling control the dynamics of gene expression. *Science* **306**, 704–708 (2004).
- [41] Tay, S. *et al.* Single-cell NF- κ B dynamics reveal digital activation and analogue information processing. *Nature* **466**, 267–271 (2010).
- [42] Li, F., Long, T., Lu, Y., Ouyang, Q. & Tang, C. The yeast cell-cycle network is robustly designed. *Proc. Natl. Acad. Sci. USA* **101**, 4781–4786 (2004).
- [43] Ferrell, J. E., Tsai, T. Y.-C. & Yang, Q. Modeling the cell cycle: why do certain circuits oscillate? *Cell* **144**, 874–885 (2011).
- [44] Lee, K., Loros, J. J. & Dunlap, J. C. Interconnected feedback loops in the Neurospora circadian system. *Science* **289**, 107–110 (2000).
- [45] Gallego, M. & Virshup, D. M. Post-translational modifications regulate the ticking of the circadian clock. *Nat. Rev. Mol. Cell Biol.* **8**, 139–148 (2007).
- [46] Meyer, T. & Stryer, L. Molecular model for receptor-stimulated calcium spiking. *Proc. Natl. Acad. Sci. USA* **85**, 5051–5055 (1988).
- [47] Qi, H., Li, X., Jin, Z., Simmen, T. & Shuai, J. The oscillation amplitude, not the frequency of cytosolic calcium, regulates apoptosis induction. *Isience* **23**, 101671 (2020).
- [48] Elowitz, M. B. & Leibler, S. A synthetic oscillatory network of transcriptional regulators. *Nature* **403**, 335 (2000).
- [49] Stricker, J. *et al.* A fast, robust and tunable synthetic gene oscillator. *Nature* **456**, 516–519 (2008).
- [50] Barnes, C. P., Silk, D. & Stumpf, M. P. Bayesian design strategies for synthetic biology. *Interface focus* **1**, 895–908 (2011).
- [51] Vellela, M. & Qian, H. On the Poincaré-Hill cycle map of rotational random walk: locating the stochastic limit cycle in a reversible Schnakenberg model. *Proceedings of the Royal Society A: Mathematical, Physical and Engineering Sciences* **466**, 771–788 (2010).
- [52] Toner, D. & Grima, R. Effects of bursty protein production on the noisy oscillatory properties of downstream pathways. *Sci. Rep.* **3**, 2438 (2013).
- [53] Qian, H. & Qian, M. Pumped biochemical reactions, nonequilibrium circulation, and stochastic resonance. *Phys. Rev. Lett.*

- 84**, 2271 (2000).
- [54] Potoyan, D. A. & Wolynes, P. G. On the dephasing of genetic oscillators. *Proc. Natl. Acad. Sci. USA* **111**, 2391–2396 (2014).
- [55] Qian, H., Saffarian, S. & Elson, E. L. Concentration fluctuations in a mesoscopic oscillating chemical reaction system. *Proc. Natl. Acad. Sci. USA* **99**, 10376–10381 (2002).
- [56] Cao, Y., Wang, H., Ouyang, Q. & Tu, Y. The free-energy cost of accurate biochemical oscillations. *Nat. Phys.* **11**, 772 (2015).
- [57] Qiao, L., Zhang, Z.-B., Zhao, W., Wei, P. & Zhang, L. Network design principle for robust oscillatory behaviors with respect to biological noise. *Elife* **11**, e76188 (2022).
- [58] Bratsun, D., Volfson, D., Tsimring, L. S. & Hasty, J. Delay-induced stochastic oscillations in gene regulation. *Proc. Natl. Acad. Sci. USA* **102**, 14593–14598 (2005).
- [59] Thomas, P., Straube, A. V. & Grima, R. The slow-scale linear noise approximation: an accurate, reduced stochastic description of biochemical networks under timescale separation conditions. *BMC Syst. Biol.* **6**, 1–23 (2012).
- [60] Thomas, P., Straube, A. V., Timmer, J., Fleck, C. & Grima, R. Signatures of nonlinearity in single cell noise-induced oscillations. *J. Theor. Biol.* **335**, 222–234 (2013).
- [61] Thomas, P., Popović, N. & Grima, R. Phenotypic switching in gene regulatory networks. *Proc. Natl. Acad. Sci. USA* **111**, 6994–6999 (2014).
- [62] Jia, C. & Grima, R. Frequency domain analysis of fluctuations of mRNA and protein copy numbers within a cell lineage: theory and experimental validation. *Physical Review X* **11**, 021032 (2021).
- [63] Jia, C., Singh, A. & Grima, R. Concentration fluctuations in growing and dividing cells: Insights into the emergence of concentration homeostasis. *PLoS Comput. Biol.* **18**, e1010574 (2022).
- [64] Gupta, A. & Khammash, M. Frequency spectra and the color of cellular noise. *Nat. Commun.* **13**, 4305 (2022).
- [65] Lestas, I., Vinnicombe, G. & Paulsson, J. Fundamental limits on the suppression of molecular fluctuations. *Nature* **467**, 174–178 (2010).
- [66] Ashall, L. *et al.* Pulsatile stimulation determines timing and specificity of NF- κ B-dependent transcription. *Science* **324**, 242–246 (2009).
- [67] Hornos, J. *et al.* Self-regulating gene: an exact solution. *Phys. Rev. E* **72**, 051907 (2005).
- [68] Grima, R., Schmidt, D. & Newman, T. Steady-state fluctuations of a genetic feedback loop: An exact solution. *J. Chem. Phys.* **137**, 035104 (2012).
- [69] Kumar, N., Platini, T. & Kulkarni, R. V. Exact distributions for stochastic gene expression models with bursting and feedback. *Phys. Rev. Lett.* **113**, 268105 (2014).
- [70] Jia, C. & Grima, R. Small protein number effects in stochastic models of autoregulated bursty gene expression. *J. Chem. Phys.* **152**, 084115 (2020).
- [71] Jia, C. & Grima, R. Dynamical phase diagram of an auto-regulating gene in fast switching conditions. *J. Chem. Phys.* **152**, 174110 (2020).
- [72] Ham, L., Schnoerr, D., Brackston, R. D. & Stumpf, M. P. Exactly solvable models of stochastic gene expression. *J. Chem. Phys.* **152**, 144106 (2020).
- [73] Cai, L., Dalal, C. K. & Elowitz, M. B. Frequency-modulated nuclear localization bursts coordinate gene regulation. *Nature* **455**, 485 (2008).
- [74] Jia, C. & Chen, Y. A second perspective on the Amann–Schmiedl–Seifert criterion for non-equilibrium in a three-state system. *J. Phys. A: Math. Theor.* **48**, 205001 (2015).
- [75] Suter, D. M. *et al.* Mammalian genes are transcribed with widely different bursting kinetics. *Science* **332**, 472–474 (2011).
- [76] Jiao, F., Sun, Q., Tang, M., Yu, J. & Zheng, B. Distribution modes and their corresponding parameter regions in stochastic gene transcription. *SIAM J. Appl. Math.* **75**, 2396–2420 (2015).
- [77] Sha, W. *et al.* Hysteresis drives cell-cycle transitions in *Xenopus laevis* egg extracts. *Proc. Natl. Acad. Sci. USA* **100**, 975–980 (2003).
- [78] Wang, J., Xu, L. & Wang, E. Potential landscape and flux framework of nonequilibrium networks: Robustness, dissipation, and coherence of biochemical oscillations. *Proc. Natl. Acad. Sci. USA* **105**, 12271–12276 (2008).